The NADES Glyceline as a Potential Green Solvent: A Comprehensive Study of its Thermophysical Properties and Effect of Water Inclusion

David Lapeña[a], Laura Lomba[a], Manuela Artal[b], Carlos Lafuente[b], Beatriz Giner[a]

[a]Universidad San Jorge. Campus Universitario, Autov A23 km 299, 50830. Villanueva de Gállego Zaragoza. Spain

[b]Departamento Química Física, Facultad de Ciencias, Universidad de Zaragoza, 50009, Zaragoza, Spain

*Corresponding author: Beatriz Giner, e-mail: bginer@usj.es, phone: 0034976060100

Abstract

In this paper, two Natural Deep Eutectic Solvents, glyceline (Gly) and glyceline-water (GlyW), containing choline chloride as acceptor H-bond compound and glycerol as donor H-bond group are studied. For glyceline the mole relation is 1 (choline chloride): 2 (glycerol) and for glyceline-water the mole relation is 1 (choline chloride) : 1.99 (glycerol) : 1.02 water. The ternary NADES has been synthetized and characterized chemically by NMR techniques for this work. Several thermophysical properties in a wide range of temperature (278.15-338.15) K and at atmospheric pressure (0.1 MPa) have been measured for both compounds: density, ρ, speed of sound, u, refractive index, n_D, surface tension,σ, isobaric molar heat capacity, $C_{p,m}$, kinematic viscosity, ν, and electric conductivity,κ. Furthermore, some related properties have been also calculated: isobaric expansibility, α_p, isentropic compressibility, κ_S, molar refraction, R_m, entropy and enthalpy of surface formationper unit surface area (ΔS_s and ΔH_s), and dynamic viscosity, η, and viscous flow and electrical conductivity activation energies. The results have been discussed in terms of the effect of temperature and the inclusion of water. We conclude that the compound containing water into the structurehas a higher molar volume and a higher fluidity. The binary NADES (Gly) is a more structured liquid than ternary one (GlyW).

Keywords:Glyceline; NADES; Thermophysical properties.

1. Introduction

Over the past two decades, the ionic liquids have been considered as the green alternative to volatile organic compounds (VOCs) due to their special properties (low volatility, high solvent capacity, and others). However, the sustainability properties of a number of ILs is not suitable from the point of view of Green Chemistry [1]. In 2004, Abbott et al [2] showed that: "the principle of creating an ionic fluid by complexing a halide salts can be applied to mixtures of quaternary ammonium salts with a range of amides" (and others hydrogen bond donors). As a consequence of the moiety process, a hydrogen-bonding network is established and the melting point decreased drastically. Relevant differences between both type of fluids, such as the synthesis method and the reactivity to water, was found and a new term, Deep Eutectic Solvent (DES), was introduced. This concept does not imply that the mixture composition corresponds to the system eutectic point. To highlight, a supramolecular structure has been detected from FT-IR, NOESY, and DOSY experiments showing that DESs are singular compounds [3-7].

If the raw materials of DESs come from natural sources, such as sugars, organic acids or amino acids, the compound is called Natural Deep Eutectic Solvent (NADES) and are supposed to be renewable. Taking into account the similarity of properties and applications, NADESs have been described by some authors as a subclass (or analogues) of ILs [8-10]. Nevertheless, a greater future in the "Green Chemistry" field is predicted for NADESs due to their chemical nature. These compounds are being used in synthesis and shape control of metallic nanoparticles, electroplating, for gas and liquid adsorption processes or as intermediate for organic chemicals synthesis, among many others uses [11].

Water in DESs can be intentionally added in order to modulate the solvent properties as absorption capacity, CO_2 solubility, and viscosity improving its potential services or applications [12,13]. Furthermore, the presence of water profoundly affects the molecular structure of the system; a structure transition from the water-NADES mixture to a type aqueous solution structure of solvated components is found when increasing the water content [14-17]. Water, at low quantity, contributes to the hydrogen-bonding network strengthens. Increasing water content, the DESs structure remains but is weakened. A significant dilution (upper than 50% water mole fraction for reline, glyceline or ethaline [16] provokes the full loss of the clusters. Besides, the water content at which this transition occurs depends strongly on the molecules and compositions of the NADESs and thus, experimentation is needed to get this information [17].

One of the most promising NADES is glyceline (Gly). This moiety is formed by choline chloride (HBA) and glycerol (HBD) in proportion, mole relation 1:2, very close to the eutectic point of the mixture($x_{\text{glycerol}} \cong 0.7, T_f \cong 230$ K)[18]. Glyceline can be used in many applications. For instance, in catalytic reactions of compounds with therapeutic properties, such as N-phenyl phthalimide derivatives, which are used as anticonvulsants and anti-inflammatory drugs [19] or extraction [20] and enzyme stabilization agent [21]. Other applications are related with the purification of (bio)fuels [22-23] or absorption processes of CO_2 and SO_2 [24] Besides, different studies about the (eco)toxicity of Gly have shown that it is relatively safe for human health and environment [25]. For instance, cytotoxicity of Gly in several line cells such as CCO or MCF-7 is quite low (EC_{50} values higher than 2000 mg·dm^3) [26] as well as its toxicity towards fungi *Aspergillus niger* and fishes *Cyprinus carpio* [27,28]. Another important finding is the relationship between the toxicity of several NADESs, including Gly, and

several physicochemical properties such as viscosity [29]. This type of connections has also been mathematically described for some ILs and the toxicity exhibited by environmental biomodels such as *Vibrio fischeri* and *Daphnia magna* [30]. Regarding biodegradability, Gly exhibits more than 90% of biodegradation at the test conditions measured, thus, this NADES can be referred to as "readily biodegradable" [25,27].

To sum up, we can say that glyceline shows interesting properties from the Green Chemistry point of view; it can be used for interesting well-stablished applications and shows a great potential for many more to find out, comes from renewable resources, presents low VOC character, is biodegradable and although more study is required, first approximations to toxicity are promising and a low (eco)toxicity profile is expected. However, with the double aim of ensuring the greenness character of Gly and using it in any reliable cost-effective process chemical process, accurate information of its thermophysical behaviour in a wide range of temperature is needed. Furthermore, there are properties that provide information about the molecular behavior of this solvent when interacting with other substances which might be in the medium that are also of great importance in order to explore and understand its molecular behaviour and make available new and useful applications [31,32]. In the literature, several papers reporting thermophysical properties of pure glyceline [33-44] and its mixtures with water [16,42-46] or other NADESs [47,48] can be found. It is worth mentioning the recent work of Troter et al [49], in this contribution, which reports the water content of compounds, density, dynamic viscosity, electrical conductivity and refractive index of some choline chloride-based deep eutectic solvents are presented. Thus, in general terms, the thermophysical information about glyceline is limited and disjointed.

For these reasons, in this manuscript we present a complete set of thermophysics properties of glyceline (Gly) over a wide range of temperature (278.15 to 338.15 K) at

atmospheric pressure. In order to explore the changes in the behaviour caused by the inclusion of water, a new NADES, glyceline-water (GlyW) formed by choline chloride, glycerol and water (mole relation 1:1.99:1.02) has been synthesized and studied; this compound is not an aqueous solution. The properties of this NADES, whose $T_f = 171.6$ K [5], have been also measured and compared with glyceline. Concretely, information about density, isobaric expansibility, speed of sound, isentropic compressibility, refractive index, molar refraction, surface tension surface, entropy and enthalpy of surface formation, isobaric molar heat capacity, kinematic and dynamic viscosity and electric conductivity, has been provided.

2. Experimental

2.1. Materials

The chemical structures of the compounds used in this work are shown in Figure S1 of the supplementary material. The information about the chemicals is presented in Table 1. The solvent glyceline was dried under vacuum for 24 hours before utilization. The water content was determined by Karl Fischer method (automatic titrator Crison KF 1S-2B). The ternary NADES, GlyW, was obtained from choline chloride, glycerol and distilled deionized water with resistivity less than 18.2 MΩ·cm. The ternary eutectic mixture was prepared by heating at T =323.15 K under continuously magnetic agitation until a colorless and homogeneous liquid is formed (about 30 minutes). The involved compounds were previously weighted in the adequate proportion using a Sartorious semi micro balance CP225D with a precision of ± 10^{-5} g. The mole relation for the choline chloride:glycerol:water is (1:1.99:1.02), this mole ratio has been calculated taking into account the water contents of choline chloride and glycerol.

2.2. Methods

2.2.1. NMR Measurements.

NMR experiments were performed on a Bruker AVANCE operating at 400 MHz for ^{1}H using a 5-mm broadband probe with z-axis gradients. The sample temperature was established at T = 298.15 K. The chemical shifts were referenced to TMS as external standard. ^{1}H-NMR spectra were recorded with a standard one-pulse sequence with 90º flip angle for excitation, with a spectral width of 16 ppm, centred at 5 ppm, 16 K data points amd relaxation time fixed to 30 s. 8 scans were acquired for the spectrum. ^{13}C-NMR spectra were recorded with an APT sequence (Bruker pulse program jmod), with a spectral width of 240 ppm, centred at 110 ppm, 64 K data points and relaxation time fixed to 2 s. 256 scans were acquired for each spectrum.

2.2.2. Thermophysical Properties.

Measurements were carried outin the temperature range (278.15 - 338.15) K in steps of 2.5 K, except in the case of refractive index, whose measurements start at T = 283.15 K.

Densities, ρ, and speed of sounds, u, were obtained simultaneously with an Anton Paar DSA 5000 vibrating tube densimeter and sound analyser (working at around 3 MHz), internally controlled at ± 0.005 K. The calibration was made using dry air and ultrapure water, supplied by SH Calibration Service GmbH. The density calibration was checked by measuring dichlorometane, a fluid denser (ρ = 1316.2 kg·m^{-3} at T =298.15 K) than water, our results are in excellent agreement with density literature data [50] for this chemical over the whole temperature range, being the average absolute deviation lower than 0.1 kg·m^{-3}. On the other hand, the Anton Paar DSA 5000 automatically corrects viscosity related errors in the density. The uncertainty of density and speed of sound can be estimated, respectively, in 0.5 kg·m^{-3} and 0.5 m·s^{-1}.

Refractive indices at 589.3 nm sodium D wavelength, n_D, were measured by means of a refractometer Abbemat-HP DR. Kernchen whose temperature was automatically thermostated within ± 0.01 K. The uncertainty of the measurements is 10^{-4}.

Surface tensions, σ, were measuredby using a drop volume tensiometer Lauda TVT-2.By means of an external Lauda E-200 thermostat, the temperature was kept constant within ± 0.01 K. The uncertainty of the surface tension measurement is 0.2 $mN \cdot m^{-1}$.

A DSC Q2000 calorimeter from TA Instrumentswas used to determine the isobaric heat capacities, $C_{p,m}$. The calorimeter measures the energy absorbed or released by a sample as it is heated, cooled, or held at constant temperature. The temperature and energy calibrations of the instrument were conducted using a standard indium sample.Heat capacity measurement was performed following the zero-heat flow procedure recommended by TA Instruments. A synthetic sapphire sample was used as reference for the heat capacities measurements. The uncertainty of the molar heat capacity measurements is1 %.

Kinematic viscosities, ν, were determined by using a Schoot-GeräteAVS-440 automatic measuring unit along with several Ubbelohde capillary viscosimeters. The uncertainty of the time flow measurements is 0.01 s, kinetic energy corrections were applied to the experimental data. The temperature was controlled within ± 0.01 K by means of a Schoot-Geräte CT 1150/2 thermostat. Dynamic viscosity, η, can be obtainedfrom density and kinematic viscosity; the estimated uncertaintyfor viscosity is 2 %.

Finally, electrical conductivities, κ, were determined using a conductimeter from CRISON, model GLP31, the conductimeter operates at alternating frequency (2 kHz).

The temperature of the sample was thermostated to ±0.01 K by means of a Lauda E-200 thermostat. The conductivity cell was calibrated with KCl aqueous solutions supplied by CRISON. The uncertainty of the measurements is 2 %.

3. Results and discussion

3.1. NMR characterization

The chemical structure of the GlyW eutectic solvent synthetized in this work was analyzed by NMR spectroscopy. ^{1}H and ^{13}C spectra, which allowed identifying the different atoms present in the compound, are presented. The corresponding structure for the binary compound, Gly, has been already elucidated in the literature by several authors[7,39,51].

The ^{1}H-NMR spectrum of the pure ternary eutectic is shown in Figure S2 of the supplementary material, all the signals are separated, except the CH_2-N^+ of choline and two CH_2OH of glycerol, which appear overlapping(Figure S2a). As regards the ^{13}C spectrum, the expected signals are obtained. Correlations between the hydroxyl hydrogens with the carbons to which they are attached are observed, indicating a slow exchange(Figure S2b).The chemical shifts, at T =298.15 K, are reported in ppm: ^{1}H-NMR: δ = 3.04 (s, 9 H, H_d), 3.23-3.33 (m, 4 H, H_f), 3.33-3.43 (m, 6 H, H, H_c), 3.44-3.53 (m, 2 H, H_g), 3.76-3.85 (m, 2 H, H_b), 4.26 (s, 2.0 H, H_i), 4.73 (t, J = 5.0 Hz, 4 $H_{f'}$, H_e), 4.82 (d, J = 4.8 Hz, 2 H, H_h), 5.08 (t, J = 4.7 Hz, 1 H, H_a); ^{13}C-NMR: δ = 53.9 (t, J = 3.0 Hz, C_d), 55.9 (C_b), 63.1 (C_f), 67.5 (C_c), 72.6 (C_g).

The previously mentioned mole ratio for GlyW has been confirmed by the ^{1}H-NMR results.

3.2. Thermophysical properties

Experimental values of density, ρ, speed of sound, u, refractive index, n_D, surface tension,σ, isobaric molar heat capacity, $C_{p,m}$, kinematic viscosity, ν, and electrical conductivity, κ, along with isentropic compressibility, κ_S, molar refraction, R_m, and dynamic viscosity, η, of Gly and GlyW are collected in TablesS1 and S2 of the supplementary material. In Figures 1-7 the variation of these properties with temperature is shown.

A lineal dependence of density, speed of sound, refractive index, surface tension and isobaric molar heat capacity with temperature has been found:

$$Y = A \cdot T + B \quad (1)$$

where Y is the studied property.The best linear fitting parameters, A and B, and the relative root-mean square deviations, $RMSDr$, between experimental and correlated data calculated using equation 2 are reported in Table 2.

$$RMSDr(\%) = 100\left(\frac{1}{n}\sum_{i=1}^{n}\left(\frac{Y_i^{exp} - Y_i^{cal}}{Y_i^{exp}}\right)^2\right)^{1/2} \quad (2)$$

The evaluation of density, speed of sound and refractive index provides general information about the molecular organization [52]. The macroscopic values obtained in these properties are the result of the balance between two principal factors: molecular structure and intermolecular interactions. So, effects related with size, shape, molecular packing and disposition of molecules are mainly reflected in volumetric properties [3].

The inclusion of water to form the new NADES, produces a decrease in density; glyceline is about 1 % denser than glyceline-water. This behaviour has been observed before[12] and is related with the decrease of hydrogen bonds interaction betweencholine chloride and glycerol, due to the presence of water molecules, affecting in this way the molecular packing. Both systems exhibit the typical inverse relation

between density and temperature as result of the increase in the mobility of molecules and ions with temperature. The calculated isobaric expansibility, $\alpha_p = -(1/\rho)(\partial\rho/\partial T)_p$, for both binary and ternary NADES were similar: 0.466 and 0.465 kK^{-1}, respectively, at T = 298.15 K.

In relation to the speed of sound, u, comparing the measured data for our compounds at the studied temperature range, a crossing point is observed. Thus, at$T<$ 283.15 K, u (Gly) >u (GlyW) and at $T>$ 283.15 K, the trend is opposite.

From density and speed of sound values and supposing that ultrasonic absorption is negligible the isentropic compressibility, κ_S, can be obtained ($\kappa_S = 1/(\rho \cdot u^2)$).This property is related to the internal structuration of the fluid: a more packed fluid has a lower value. As expected, $\kappa_S$increase with temperature, following the general behaviour of liquids. We can see that including water in the structure, GlyW, the isentropic compressibility is increased. Once again, results indicate that the ternary NADES exhibits a less packed structure.

We have also calculated from density and refractive index the molar refraction, R_m, by using the Lorentz–Lorenz relation:

$$R_m = \frac{M \cdot (n_D^2 - 1)}{\rho \cdot (n_D^2 + 2)} \quad (3)$$

where M is the molar mass of the corresponding NADES. Refractive index values decrease and molar refraction increases when the temperature increases. Both properties are lower in the GlyW compound. The unoccupied volume or free molar volume, can be easily obtained since $R_m$is associated to the hard core volume of the system [54]. AtT = 298.15 K, the estimated free volume/molar volume ratio for Gly and GlyW are 0.649 and 0.717. Results corroborate the less packed structure when water is included into the system.

Surface tension, σ, is related to the extent of the intermolecular interactions between the molecules of a substance. The energy of the molecules sited within the bulk is lower than that of the surface ones due to the compensation of intermolecular forces and, therefore, tend to stay there.The stronger the intermolecular interactions, the higher the energy needed to move a molecule to the surface; that is, the surface tension is higher. According to this, results indicate that GlyW presents slightly stronger interactions than Gly. This effect is small but significant and is probably due to the higher hydrogen bond number in the ternary NADES.This property is profoundly affected by the temperature changes because the intermolecular interactions considerably vary with them. A similar behaviourwith the temperature for both compounds is observed. In order to get information about the distribution of molecules in the surface, entropy ofsurface formationper unit surface area, $\Delta S_s = -(\partial\sigma/\partial T)_p$), and enthalpyofsurface formationper unit surface area, $\Delta H_s = \sigma - T(\partial\sigma/\partial T)_p$, have been obtained. Due to the lineal relationship between σ and temperature, the entropyof surface formation per unit surface area, ΔS_s,is constant withtemperature and the calculated values for Gly and GlyW were0.0531and 0.0503 $mN^{-1}\cdot m^{-1}\cdot K^{-1}$, respectively.Taking account these values, at$T$ = 298.15 K, ΔH_s = 82.78 $mN^{-1}\cdot m^{-1}$for Gly and ΔH_s = 83.39$mN^{-1}\cdot m^{-1}$for GlyW. The lowerΔS_s and ΔH_svalues the higher the orientation degree in the surface [55]. So, Gly is a more structured liquid than GlyW.

Information obtained from thermal properties such as isobaric molar heat capacity, $C_{p,m}$, is important in setting of industrial processes and operation conditions. Molar heat capacity values increase with temperature for both studied systems and no anomalous behaviour is noticed. Heat capacity values are lower for the ternary compound.

Many potential industrial applications of NADES depend on their transport properties and their rheological behaviour. For instance, several ionic mixtures have viscosity indexes superior to many mineral base oils and thus, can be used as lubricants [56]or for electrodeposition processes. Dynamic viscosity, η, is calculated from the experimental density and kinematic viscosity ($\eta = \rho \cdot \nu$). The inclusion of water produces an accused decrease of the dynamic viscosity values. As we have previously pointed out, the presence of water molecules produces an increase in the extent of intermolecular interactions. Thus, viscosity reflects in this case, the modifications in the structure and packing. The behaviour against the temperature is the expected (values dramatically decrease with temperature). In fact, the relationship between η and temperature can be correlated using the exponential Vogel-Fulcher-Tamman equation[57-59]:

$$\eta = \eta_0 exp[B/(T - T_0)] \quad (4)$$

where η_0, B and T_0 are the adjustable parameters, which are included in Table 1 along with the corresponding relative root-mean square deviations. The B parameter is related with the activation energy of viscous flow. Lower values in this activation energy correspond to ions with higher mobility of particles within the melt.In our study, this parameter decreases with water content. Once again, the inclusion of water affects profoundly the structure of the NADES and produces an increase in the volume, leading to a less packed structure where molecules and ions with higher mobility degree.

The electric conductivity, κ, is higher when water is included into the moiety. It can observe the influence of the temperature on κ for the studied NADESs. This dependence follows an equation similar to the previous one but the sign inside the exponential part is contrary because the electrical conductivityincreases with temperature:

$$\kappa = \kappa_0 exp[-B/(T - T_0)] \quad (5)$$

where κ_0, B and T_0 are the adjustable parameters, these parameters and relative root-mean square deviations, are collected in Table 1. Analogously to the previous analysis, B is related with the activation energy for electrical conductivity. This parameter is lower in GlyW.

Table 3 shows the comparison of our thermophysical results for glyceline with previously reported values.

There are a lot of works reporting the density of glyceline [16, 33-39, 42, 43, 45, 48, 49]. Most of them present density values slightly lower than our experimental ones. Nevertheless two of them [33, 35] give densities higher than ours. It is worth mentioning that our isobaric expansibilities agree very well with the calculated ones from density data of all these papers, except the α_p calculated using the reported densities by Troter et al. [49]. The deviation of our speed of sound measurements with those of Mjalli et al. [33] is very high (Δu = 103 m·s^{-1}); at low temperatures our u values are lower while at high temperatures are higher. At T = 298.15 K the deviation is only 7.7 m·s^{-1}. Published refractive indices [36, 43, 44] are higher than our values, the n_D values of Troter et al. [49] are also higher but at low temperatures are closer. Finally the refractive index at T = 298.15 K reported by Shahbaz et al. [38] and the n_D data of Mjalli et al. [48] are very similar to our experimental refractive indices. The surface tensions obtained in this work for glyceline are higher than previously published values, although the σ value at T = 298.15 K reported by Abbott et al. [34] is only slightly higher than our value. There is only a paper reporting isobaric molar heat capacity, our values are lower than the results of Leron et al [46]. Regarding the viscosity data, the viscosities here presented are higher than the values reported by Mjalli et al. [33, 48] but lower than the results of Troter et al. [49] at low temperatures. With respect to the rest

of literature data, our η values are not very far. In this sense, it can be pointed out that our results agree very well with those of Chemat et al. [36] and Yadav et al. [45]. With respect to conductivity results our values are higher than conductivity data of AlOmar et al. [35] and Troter et al. [49] especially at higher temperatures. The κ values of Mjalli et al. [48] are higher than ours at low temperatures and very similar at high temperatures. On the other hand, the conductivities reported by Bagh et al. [41] agree a little better with our results.

Finally, no data were found for the glyceline-water NADES with the exact water content of this work (0.255 in mole fraction). Figure 8 shows the comparison between our data and those published for the glyceline-water system. Density data are in agreement with the literature although Yadav et al. [45] data at T > 303 K are slightly lower than the rest. It can be seen that our refractive indices are slightly higher than Leron et al. [43] ones. On the other hand, our isobaric molar heat capacity and those from Leron et al. [46] are in very well agree as the Figure 8 indicates. Last, the comparison of experimental viscosity data (this work) with the literature [45] is better at higher temperatures.

4. Conclusions

In this contribution a comprehensive thermophysical characterization of two NADESs (glyceline and glyceline-water) based on choline chloride and glycerol is presented. The ternary NADES, glyceline-water, (mole relation 1:1.99:1.02) has been synthetized and characterized chemically by NMR spectroscopy. The properties measured in a wide range of temperatures (278.15-338.15) K at atmospheric pressure were: density, speed of sound, refractiveindex, surface tension, isobaric molar heat capacity,viscosity, and electrical conductivity. The effect on the thermophysical

properties of NADESs of both temperature and inclusion of waterhas been analyzed. The temperature behavior of the studied properties for both NADESs is the expected.It can be outlined that effect of water inclusion is not appreciable on speed of sound and isentropic compressibility values. For the rest of properties, the water inclusion plays an important role; the NADES glyceline-water presents a higher molar volume and a higher fluidity.

Conflicts of interest

There are no conflicts to declare.

Acknowledgments

Financial supportfrom Diputación General de Aragón (Grant E31_17R), Fondo de Desarrollo Regional “Construyendo Europa desde Aragón is gratefully acknowledged.

References

[1] A. Paiva, R. Craveiro, I. Aroso, M. Martins, R. L. Reis and A. R. C. Duarte. Natural deep eutectic solvents - Solvents for the 21st Century. ACS Sustain. Chem. Eng.2014, 2, 1063-1071.

[2] A. P. Abbott, D. Boothby, G. Capper, D.L. Davies, R.K. Rasheed. Deep eutectic solvents formed between choline chloride andcarboxylic acids: versatile alternatives to ionic liquids. J. Amer. Chem. Soc. 2004, 126, 9142-9147.

[3] C. D'Agostino, R.C. Harris, A.P. Abbott, L.F. Gladden, M.D. Mantle. Molecular motion and ion diffusion in choline chloride based deep eutectic solvents studied by 1H pulsed field gradient NMR spectroscopy. Phys. Chem. Chem. Phys. 2011, 13, 21383-21391.

[4] M. Francisco, A. van den Bruinhorst, M.C. Kroon. New natural and renewable low transition temperature mixtures (LTTMs): screening as solvents for lignocellulosic biomass processing. Green Chem. 2012, 14, 2153-2157.

[5] Y. Dai, J. van Spronsen, G. J. Witkamp, R. Verpoorte, Y. H. Choi. Natural deep eutectic solvents as new potential media for greentechnology. Anal. Chim. Acta 2013, 766, 61-68.

[6] C. Florindo, F.S. Oliveira, L.P.N. Rebelo, A.M. Fernandes, I.M. Marrucho. Insights into the synthesis and properties of deep eutectic solvents based on cholinium chloride and carboxylic acids. ACS Sustain. Chem. Eng. 2014, 2, 2416-2425.

[7] R. Stefanovic, M. Ludwig, G.B. Webber, R. Atkin, A.J. Page. Nanostructure, hydrogen bonding and rheology in choline chloride deep eutectic solvents as a function of the hydrogen bond donor. Phys. Chem. Chem. Phys. 2017, 19, 3297-3306.

[8] P. Dominguez de María, Z. Maugeri. Ionic liquids in biotransformations: from proof-of-concept to emerging deep-eutectic-solvents. Curr. Op. Chem. Biol. 2011, 15, 220-225.

[9] A. Shishov, A. Bulatov, M. Locatelli, S. Carradori, V. Andruch. Application of deep eutectic solvents in analytical chemistry. A review. Microchem. J. 2017, 135, 33-38.

[10] F. S. Mjalli, H. Mousa. Viscosity of aqueous ionic liquids analogues as a function of water content and temperature. Chin. J. Chem. Eng. 2017, 25, 1877-1883.

[11] M. Espino, M.A. Fernandez, F.J.V. Gomez, M.F. Silva.Natural designer solvents for greening analytical chemistry. Trends Anal. Chem. 2016, 76, 126-136.

[12] V. S. Protsenko, A. Kityk, D.A. Shaiderov, F.I. Danilov. Effect of water content on physicochemical properties and electrochemical behavior of ionic liquids containing choline chloride, ethylene glycol and hydrated nickel chloride. J.Mol. Liq. 2015, 212, 716-722.

[13] D. Shah, F. S. Mjalli, Effect of water on the thermo-physical properties of Reline: An experimental and molecular simulation based approach. Phys. Chem. Chem. Phys. 2014, 16, 23900-23907.

[14] Y. Dai, G.J. Witkamp, R. Verpoorte, Y.H. Choi. Tailoring properties of natural deep eutectic solvents with water to facilitate their applications. Food Chem. 2015, 187, 14-19.

[15] E. Duran, J. Lecomte, P. Villeneuve. From green chemistry to nature: The versatile role of low transition temperature mixtures. Biochimie 2016, 120, 119-123.

[16] T. Zhekenov, N. Toksanbayev, Z. Kazakbaveva, D. Shah, F.S. Mjalli. Formation of type III Deep Eutectic Solvents and effect of water on their intermolecular interactions. Fluid Phase Eq. 2017, 441, 43-48.

[17] O. S. Hammond, D. T. Bowron, K. J. Edler. The effect of water upon deep eutectic solvent nanostructure: An unusual transition from ionic mixture to aqueous solution. Angew. Chem. Int. Ed. 2017, 56, 9782-9785.

[18] A. P. Abbott, P. M. Cullis, M. J. Gibson, R. C. Harris, E. Raven. Extraction of glycerol from biodiesel into a eutectic based ionic liquid. Green Chem. 2007, 9, 868-872.

[19] H. R. Lobo, B. S. Singh, G. S. Shankarling. Deep eutectic solvents and glycerol: a simple, environmentally benign and efficient catalyst/reaction media for synthesis of N-aryl phthalimide derivatives. Green Chem. Lett. Rev. 2012, 5, 487-533.

[20] A. K. Das, M. Sharma, D. Mondal, K. Prasad. Deep eutectic solvents as efficient solvent system for the extraction of kappa-carrageenan from Kappaphycus alvarezii. Carbohydr. Polym. 2016, 136, 930-935.

[21] S. Daneshjou, S. Khodaverdian, B. Dabirmanesh, F. Rahimi, S. Daneshjoo, F. Ghazi, K. Khajeh. Improvement of chondroitinases ABCI stability in natural deep eutectic solvents. J. Mol. Liq. 2017, 227, 21-25.

[22] C. Li, C., D. Li, S. Zou, Z. Li, J. Yin, A. Wang, Y. Cui, Z. Yao, Q. Zhao. Extraction desulfurization process of fuels with ammomiu,-based deep eutectic solvents. Green Chem. 2013, 15, 2793-2799.

[23] K. Shahbaz, F. S. Mjalli, M. A. Hashim, I.M. AlNasheff. Eutectic solvents for the removal of residual palm oil-based biodiesel catalyst. Sep. Pur. Technol. 2011, 81, 216-222.

[24] K. Mulia, S. Putri, E. Krisanti, Nasruddin. AIP in Natural deep eutectic solvents (NADES) as Green Solvents for Carbon Dioxide Capture. AIP Conference Proceedings 1823, DOI: 020022 2017. doi.org/ 10.1063/1.4978095.

[25] M. Hayyan, C.Y. Looi, A. Hayyan, W.F. Wong, M.A. Hashim. In Vitro and In Vivo toxicity prolifing of ammonium-based deep eutectic solvents. PloS One 2015, 10, DOI: e0117934.

[26] K. Radosevic, M. C. Bubalo, V. G. Srcek, D. Grgas, T.L. Dragicevic, I.R. Redovnikovic. Evaluation of toxicity and biodegradability of choline chloride based deep eutectic solvents. Ecotoxicol. Environ. Saf. 2015, 112, 46-53.

[27] I. Juneidi, M. Hayyan, O. M. Ali. Toxicity profile of choline chloride-based deep eutectic solvents for fungi and Cyprinus carpio fish. Environ. Sci. Pollut. Res. 2016, 23, 7648-7659.

[28] I. Juneidi, M. Hayyan, M. A. Hashim. Evaluation of toxicity and biodegradability for cholinium-based deep eutectic solvents. RSC Adv. 2015, 5, 83636-83647.

[29] M. Hayyan, Y. P. Mbous, C. Y. Looi, W. F. Wong, A. Hayyan, Z. Salleh, O. Mohd-Ali. Natural deep eutectic solvents: cytotoxic profile. Springerplus 2016, 5, 913.

[30] E. Perales, L. Lomba, M. García-Escudero, E. Sarasa, C.E. Lafuente, B. Giner. Toxicological study of some ionic liquids. Green Process. Synthesis 2017, DOI: doi.org/10.1515/gps-2017-0031.

[31] J. Dupont, P. A. Suarez. Z. Physico-chemical processes in imidazolium ionic liquids. Phys. Chem. Chem. Phys. 2006, 8, 2441-2452.

[32] R. P. Swatloski, A. E. Visser, W.M. Reichert, G.A. Broker, L. M. Farina, J. D. Holbrey, R. D. Rogers. On the solubilization of water with ethanol in hydrophobic hexafluorophosphate ionic liquids. Green Chem. 2002, 4, 81-87.

[33] F. S. Mjalli, N. M.A. Jabbar. Acoustic investigation of choline chloride based ionic liquids analogues. Fluid Phase Equilib. 2014, 381, 71-76.

[34] A. P. Abbott, A. Y. M. Al-Murshedi, O. A. O. Alshammari, R. C. Harris, J. H. Kareem, I. B. Qader, K. Ryder. Thermodynamics of phase transfer for polar molecules from alkanes to deep eutectic solvents. Fluid Phase Equilib. 2017, 448, 99-104.

[35] M. K. AlOmar, M. Hayyan, M. A. Alsaadi, S. Akib, A. Hayyan, M. A. Hashim. Glycerol-based deep eutectic solvents: Physical properties. J. Mol. Liq. 2016, 215, 98-103.

[36] F. Chemat, H. J. You, K. Muthukumar, T. Murugesan. Effect of L-arginine on the physical properties of choline chloride and glycerol based deep eutectic solvents. J. Mol. Liq. 2015, 212, 605-611.

[37] N. R. Rodriguez, J. F. Guell, M. C. Kroon. Glycerol-Based Deep Eutectic Solvents as Extractants for the Separation of MEK and Ethanol via Liquid Liquid Extraction. J. Chem. Eng. Data 2016, 61, 865-872.

[38] K. Shahbaz, F. S. G. Bagh, F. S. Mjalli, I. M. AlNashef, M. A. Hashim. Prediction of refractive index and density of deep eutectic solvents using atomic contributions. Fluid Phase Equilib. 2013, 354, 304-311.

[39] K. Shahbaz, S. Baroutian, F. S. Mjalli, M. A. Hashim, I. M. AlNashef. Densities of Ammonium and Phosphonium based Deep Eutectic Solvents: Prediction using Artificial Intelligent and Group Contribution Techniques. Thermochim. Acta 2012, 527, 59-66.

[40] F. S. Mjalli, G. Vakili-Nezhaad, K. Shahbaz, I. M. AlNashef. Application of the Eotvos and Guggenheim empirical rules for predicting the density and surface tension of ionic liquids analogues. Thermochim. Acta 2014, 575, 40-44.

[41] F. S. G. Bagh, K. Shahbaz, F. S. Mjalli, I. M. AlNashef, M. A. Hashim. Electrical conductivity of ammonium and phosphonium based deepeutectic solvents: Measurements and artificial intelligence-based prediction. Fluid Phase Equilib. 2013, 356, 30-37.

[42] R. B. Leron, D. S. H. Wong, M. H. Li. Densities of a deep eutectic solvent based on choline chloride and glycerol and its aqueous mixtures at elevated pressures. Fluid Phase Equilib. 2012, 335, 32-38.

[43] R. B. Leron, A. N. Soriano, M. H. Li. Densities and refractive indices of the deep eutectic solvents (choline chloride + ethylene glycol or glycerol) and their

aqueous mixtures at the temperature ranging from 298.15 to 333.15 K. J. Taiwan Inst. Chem. Eng. 2012, 43, 551-557.

[44] C. Ma, Y. Guo, D. Li, J. Zong, X. Ji, C. Liu. Molar enthalpy of mixing and refractive indices of choline chloride-based deep eutectic solvents with water. J. Chem. Thermodyn. 2017, 105, 30-36.

[45] A. Yadav, S. Trivedi, R. Rai, S. Pandey. Densities and dynamic viscosities of (choline chloride plus glycerol) deep eutectic solvents and its aqueous mixtures in the temperature range (283.15-363.15) K. Fluid Phase Equilib. 2014, 367, 135-142.

[46] R. B. Leron, M. H. Li. Molar heat capacities of choline chloride-based deep eutectic solvents and their binary mixtures with water. Thermochim. Acta 2012, 530, 52-57.

[47] F. S. Mjalli, O. U. Ahmed. Characteristics and intermolecular interaction of eutectic binary mixtures: Reline and Glyceline. Korean J. Chem. Eng. 2016, 33, 337-343.

[48] F. S. Mjalli, O. U. Ahmed. Ethaline and Glyceline binary eutectic mixtures: characteristics and intermolecular interactions. Asia-Pac. J. Chem. Eng. 2017, 12, 313-320.

[49] D. Z. Troter, Z. B. Todorovic, D. R. Dokic-Stojanovic, B. S.Dordevic, V. M. Todorovic, S. S. Konstantinovic, V. B. Veljkovic. The physico-chemical and thermodynamic properties of the choline chloride-based deep eutectic solvents. J. Serb. Chem. Soc. 2017, 82, 1039-1002.

[50] D.V. Wagle, G. A. Baker, E. Mamontov. Differential microscopic mobility of components within a deep eutectic solvent. J. Phys. Chem. Lett. 2015, 6, 2924-2928.

[51] TRC-Tables TRC Thermodynamic Tables, Hydrocarbons Selected Values ofProperties of Chemical Compounds; Thermodynamic Research Center; TexasA&M University, College Station, TX, 1973.

[52] B. Giner, C. Lafuente, A. Villares, M. Haro, M.C. Lopez. Volumetric and refractive properties of binary mixtures containing 1,4-dioxane and chloroalkanes. J. Chem. Thermodyn. 2007, 39, 148-157.

[53] L. Lomba, B. Giner, E. Zuriaga, I. Gascon, C. Lafuente. Thermophysical properties of lactates. Thermochim. Acta 2014, 575, 305-312.

[54] P. Brocos, A. Piñeiro, R. Bravo, A. Amigo. Refractive indices, molar volumes and molar refractions of binary liquid mixtures: concepts and correlations. Phys. Chem. Chem. Phys. 2003, 5, 550-557.

[55] L. Lomba, B. Giner, I. Bandres, C. Lafuente, M.R. Pino. Physicochemical properties of green solvents derived from biomass. Green Chem. 2011, 13, 2062-2070.

[56] A. P. Abbott, E. I. Ahmed, R. C. Harris, K. S. Ryder. Evaluating water miscible deep eutectic solvents (DESs) and ionic liquids as potential lubricants. Green Chem. 2014, 16, 4156-4161.

[57] H. Vogel. Das temperaturabhängigkeitsgesetz der viskosität von flüssigkeiten. Z. Phys. 1921, 22, 645-646.

[58] G. S. Fulcher. Analysis of recent measurements of the viscosity of glasses. Am. Ceram. Soc. J. 1925, 8, 339-355.

[59] G. Tammann, W. Hesse. Die abhängigkeit der viscosität von der temperatur bie unterkühlten flüssigkeiten. Z. Anorg. Allg. Chem. 1926, 156, 254-257.

Table 1. Sample table.

Chemical Name	Formula	CAS Number	Source	Purification method	MassFraction Purity [a]	Water content / ppm
Choline chloride	$C_5H_{14}ClNO$	67-48-1	Sigma-Aldrich		0.993	1250
Glycerol	$C_3H_8O_3$	56-81-5	Sigma-Aldrich		0.999	500
Glyceline			Scionix	Vacuum treatment	0.98	275

[a] As stated by the supplier.

Table 2. Fitting parameters along with the corresponding relative root-mean square deviations, $RMSDr$, for the measured properties.

	Property	A	B	C	$RMSDr$ / %
Gly	ρ / kg·m^{-3}	-0.557	1361.91		0.01
	u / m·s^{-1}	-2.242	2670.72		0.04
	n_D	-2.377·10^{-4}	1.55544		0.00
	σ / mN·m^{-1}	-0.053	82.80		0.06
	$C_{p,m}$ / J·mol·K^{-1}	0.332	119.5		0.05
	η [a] / mPa·s	0.0234	1362.3	155.17	0.75
	κ [b] / mS·cm^{-1}	2899.2	958.7	175.47	0.88
GlyW	ρ / kg·m^{-3}	-0.550	1346.50		0.00
	u / m·s^{-1}	-2.052	2617.74		0.02
	n_D	-2.329·10^{-4}	1.54760		0.00
	σ / mN·m^{-1}	-0.050	83.40		0.12
	$C_{p,m}$ / J·mol·K^{-1}	0.327	90.5		0.05
	η [a] / mPa·s	0.0350	1175.1	157.50	0.86
	κ [b] / mS·cm^{-1}	882.7	594.6	196.45	0.12

[a] $A = \eta_0; C = T_0$

[b] $A = \kappa_\infty; C = T_0$

Table 3. Absolute deviations, Δy, and relative root-mean-square deviations, *RMSDr*, between our experimental and literature data for Gly (choline chloride (ChCl) + glycerol).

Reference	Water content / ppm	x_{ChCl}	ρ / kg·m^{-3}		u / m·s^{-1}		n_D		σ / mN·m^{-1}		$C_{p.m}$ / J·mol^{-1}·K^{-1}		η / mPa·s		κ / mS·cm^{-1}	
			$\Delta\rho$	$RMSD_r$ / %	Δu	$RMSD_r$ / %	Δn_D	$RMSD_r$ / %	$\Delta\sigma$	$RMSD_r$ / %	$\Delta C_{p.m}$	$RMSD_r$ / %	$\Delta\eta$	$RMSD_r$ / %	$\Delta\kappa$	$RMSD_r$ / %
Zhekenov [16]		0.33	4.38	0.37												
Mjalli [33]	2000	0.33	18.79	1.56	103.46	6.11			10.22	10.38			60.65	23.42		
Abbott [34]		0.333							1.75	2.55			23.65	7.99		
AlOmar [35]		0.333	13.10	1.10					10.56	19.29			14.93	15.64	1.80	78.06
Chemat [36]		0.333	4.91	0.42			0.0024	0.16					5.33	4.72		
Rodríguez [37]	3000	0.333	4.75	0.40									30.31	12.63		
Shahbaz [38]		0.34	1.17	0.10			0.0006	0.04								
Shahbaz [39]	1000	0.33	3.36	0.28												
Mjalli [40]		0.33							10.24	18.36						
Bagh [41]		0.34													0.46	16.13
Leron [42]	392	0.333	3.93	0.33												
Leron [43]	2000	0.333	4.51	0.38			0.0023	0.15								
Ma [44]		0.333					0.0019	0.13								
Yadav [45]		0.333	4.56	0.39									11.17	4.65		
Leron [46]	1500	0.333									17	7.02				
Mjalli [48]	100	0.333	5.19	0.44			0.0006	0.05					33.80	22.18	0.72	34.00
Troter [49]	350	0.333	6.60	0.5999			0.0014	0.10					49.57	17.22	0.75	27.69

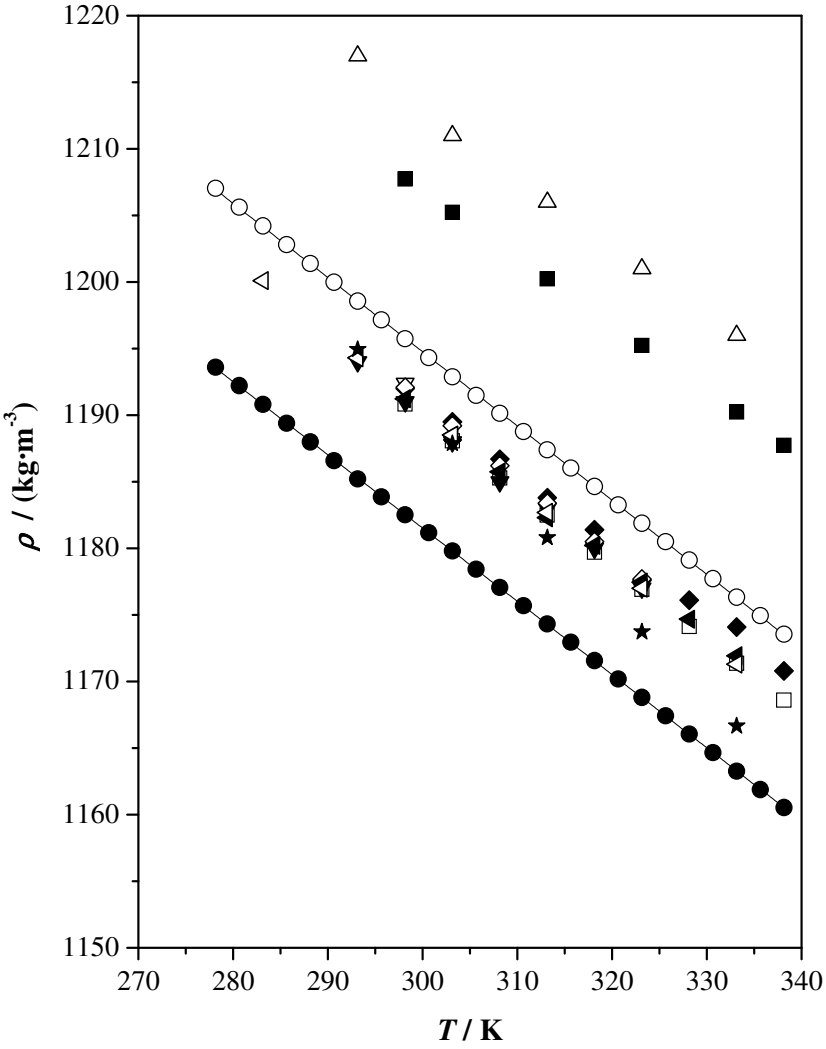

Figure 1. Density, ρ, as a function of temperature, T, at p = 0.1 MPa for the studied compounds. Gly: (○) experimental; (▲) Ref. [16]; (△) Ref. [33]; (■) Ref. [35]; (□) Ref. [36]; (▼) Ref. [37]; (▽) Ref. [38]; (◆) Ref. [39]; (◇) Ref. [42]; (◄) Ref. [43]; (◁) Ref. [45]; (★) Ref. [48]; (☆) Ref. [49]. GlyW: (●) experimental.

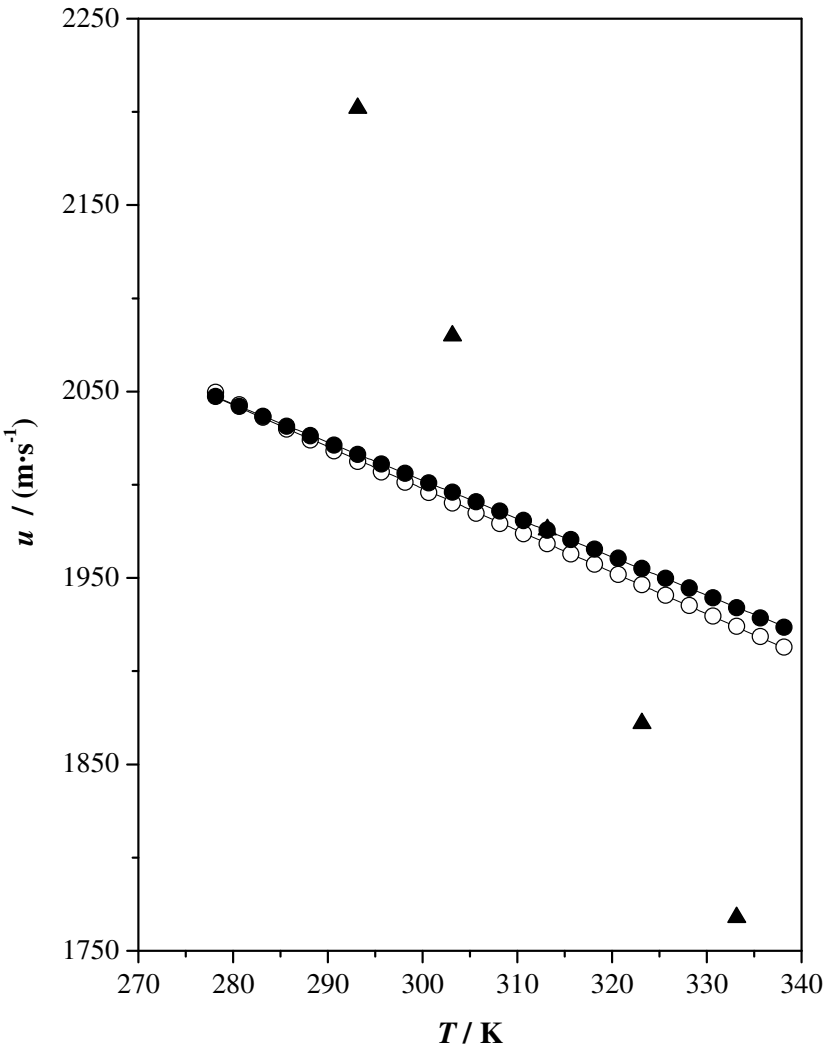

Figure 2. Speed of sound, u, as a function of temperature, T, at p = 0.1 MPa for the studied compounds. Gly: (○) experimental; (▲) Ref. [33]. GlyW: (●) experimental.

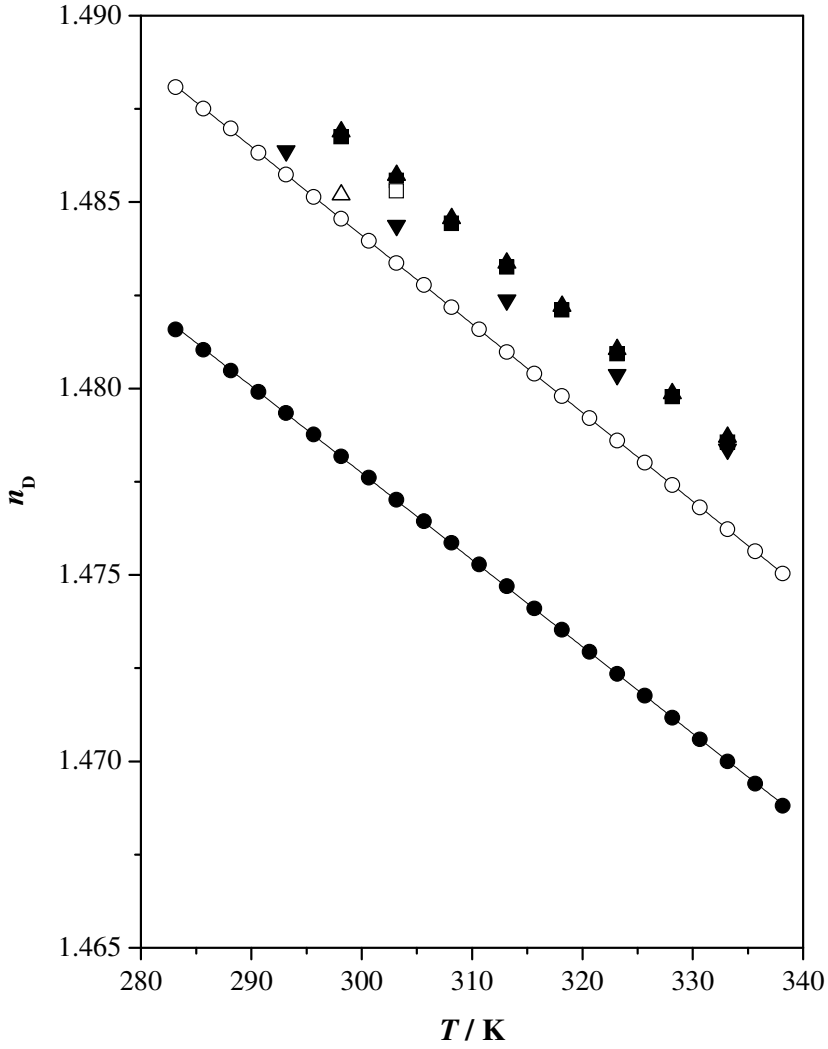

Figure 3. Refractive index, n_D, as a function of temperature, T, at p = 0.1 MPa for the studied compounds. Gly: (○) experimental; (▲) Ref. [36]; (△) Ref. [38]; (■) Ref. [43]; (□) Ref. [44]; (▼) Ref. [48]; (▽) Ref. [49]. GlyW: (●) experimental.

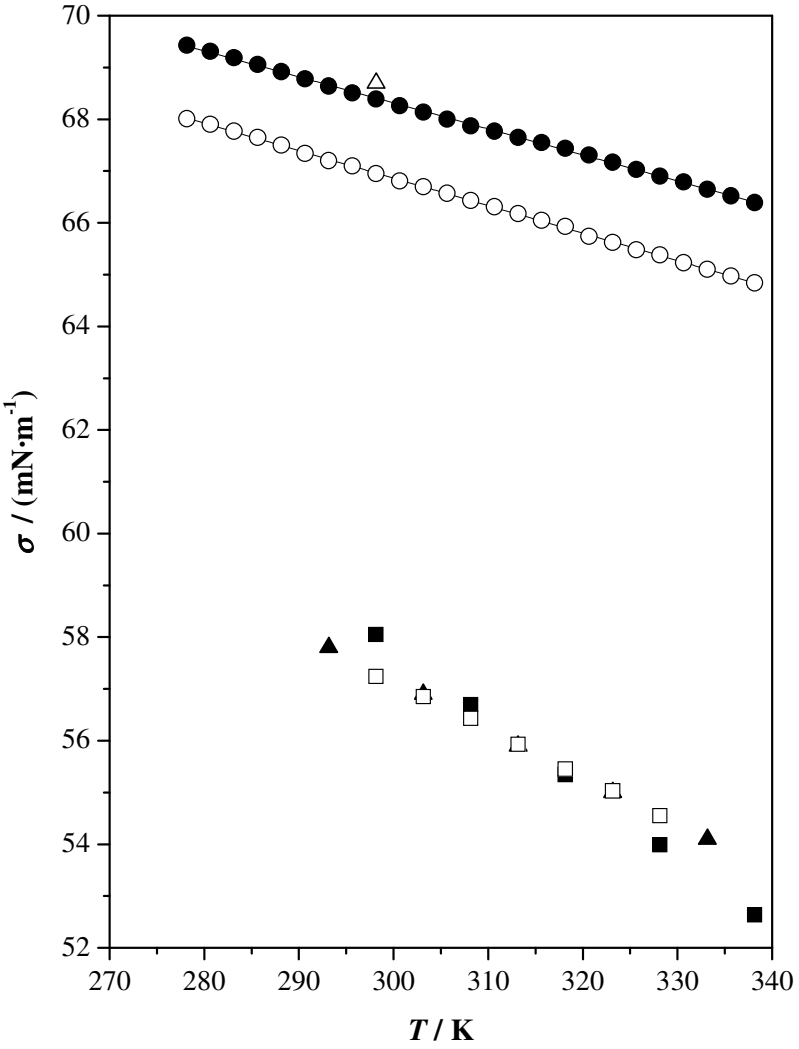

Figure 4. Surface tension, σ, as a function of temperature, T, at p = 0.1 MPa for the studied compounds. Gly: (○) experimental; (▲) Ref. [33]; (△) Ref. [34]; (■) Ref. [35]; (□) Ref. [40]. GlyW: (●) experimental.

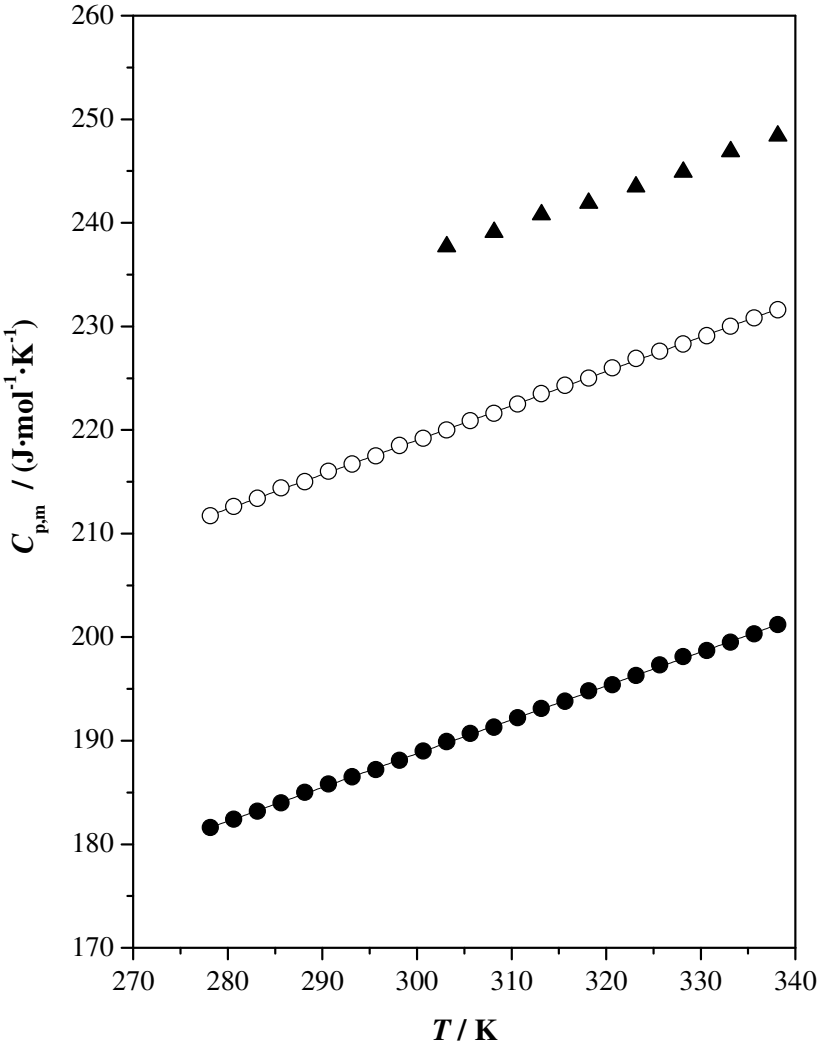

Figure 5. Isobaric molar heat capacity, $C_{p,m}$, as a function of temperature, T, at p = 0.1 MPa for the studied compounds. Gly: (○) experimental; (▲) Ref. [46]. GlyW: (●) experimental.

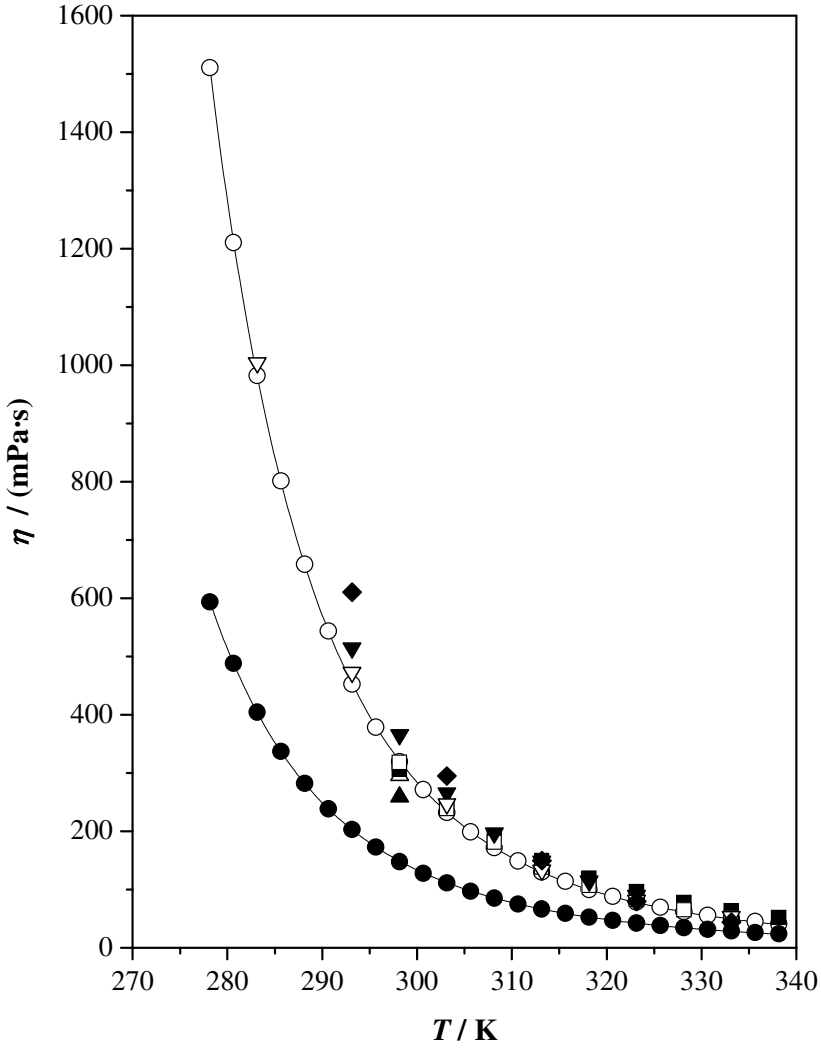

Figure 6. Dynamic viscosity, η, as a function of temperature, T, at p = 0.1 MPa for the studied compounds. Gly: (○) experimental; (▲) Ref. [33]; (△) Ref. [34]; (■) Ref. [35]; (□) Ref. [36]; (▼) Ref. [37]; (▽) Ref. [45]; (◆) Ref. [48]; (◇) Ref. [49]. GlyW: (●) experimental.

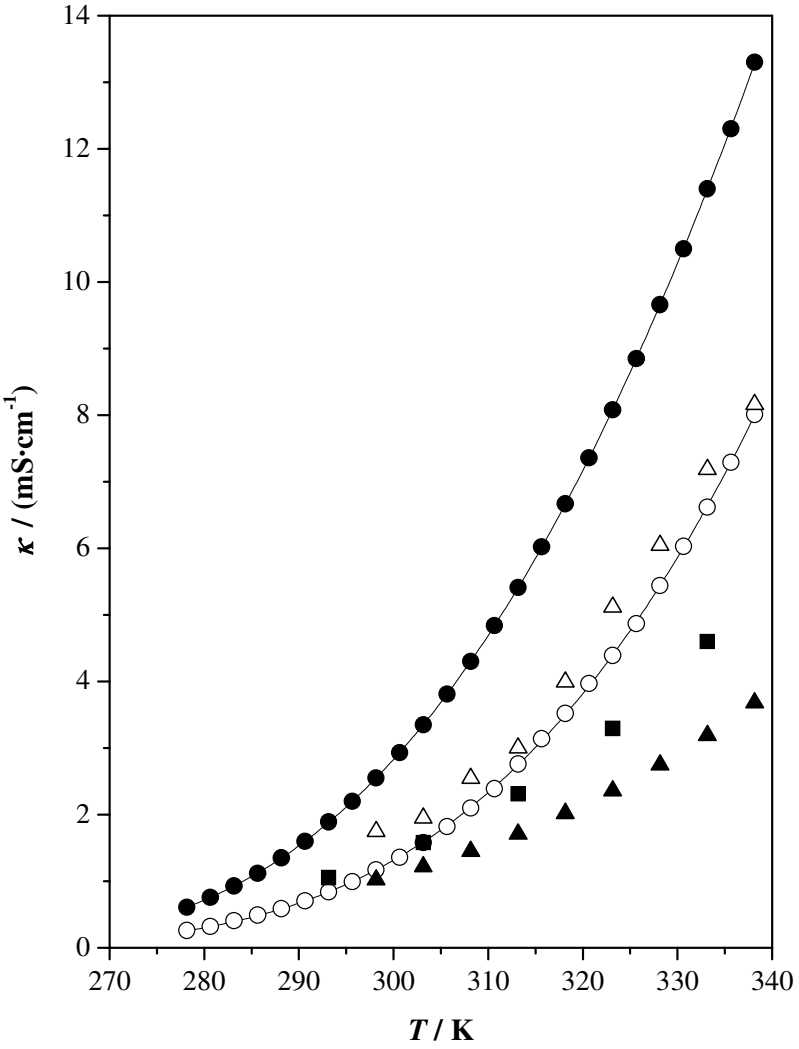

Figure 7. Electrical conductivity, κ, as a function of temperature, T, at p = 0.1 MPa for the studied compounds. Gly: (○) experimental; (▲) Ref. [35] ; (△) Ref. [41]; (■) Ref. [48]; (□) Ref. [49]. GlyW: (●) experimental.

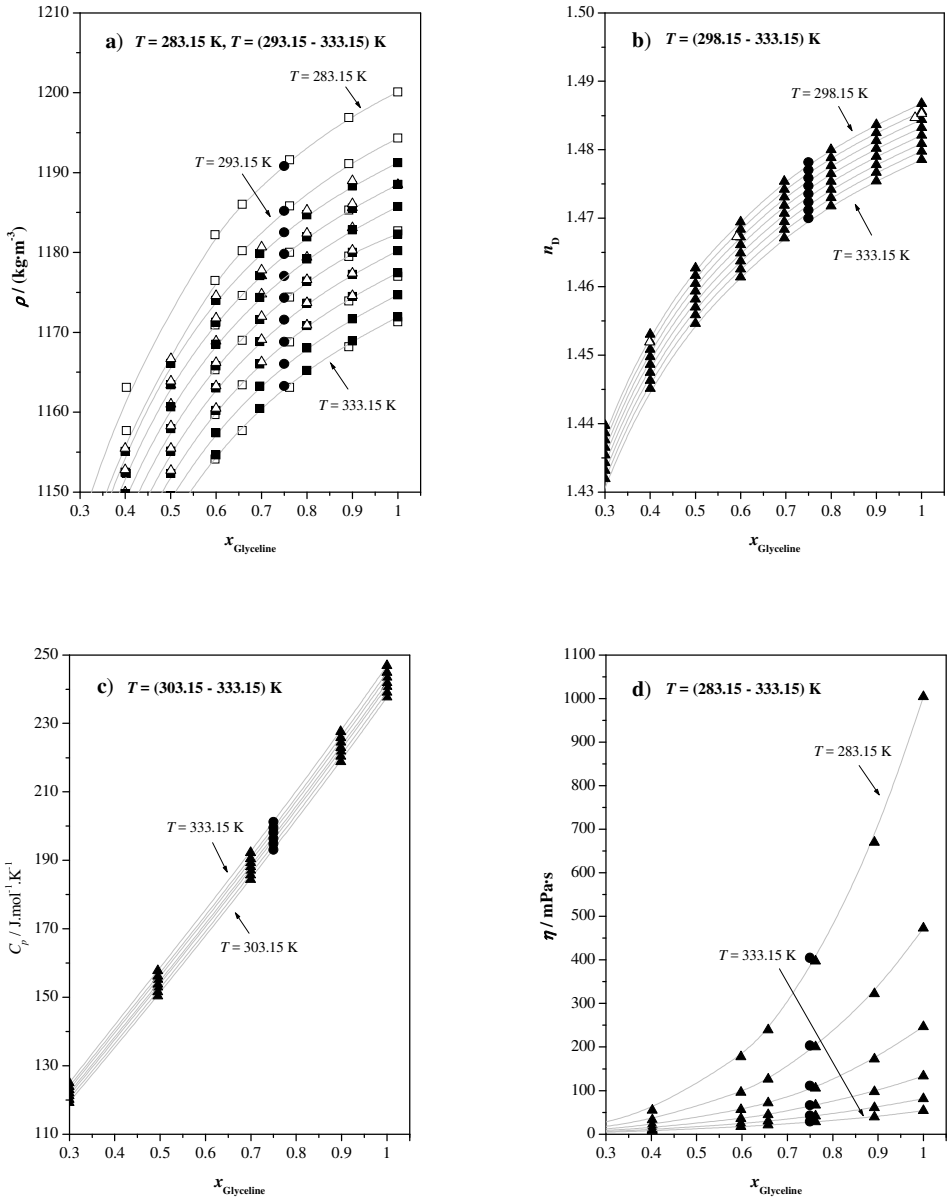

Figure 8. Comparison between our experimental and literature data for several thermophysical properties for GlyW. (a), Density, ρ: (●), this work; (▲), Ref. [16]; (△), Ref. [42]; (■), ref. [43]; (□), Ref. [15]. (b) Refractive index, n_D: (●), this work; (▲), Ref. [43]; (△), ref. [44]. (c), Isobaric molar heat capacity, $C_{p,m}$: (●), this work; (▲), Ref. [46]. (d), Dynamic viscosity, η: (●), this work; (▲), Ref. [45].

SUPPLEMENTARY MATERIAL

The NADES glyceline as a potential green solvent: a comprehensive study of its physicochemical properties and effect of water inclusion

David Lapeña[a], Laura Lomba[a], Manuela Artal[b], Carlos Lafuente[b], Beatriz Giner[a]

[a]Universidad San Jorge. Campus Universitario, Autov A23 km 299, 50830. Villanueva de Gállego Zaragoza. Spain

[b]Departamento Química Orgánica-Química Física, Facultad de Ciencias, Universidad de Zaragoza, 50009, Zaragoza, Spain

*Corresponding author: Beatriz Giner, e-mail: bginer@usj.es, phone: 0034976060100

Table S1. Experimental and derived thermophysical properties of glyceline (choline chloride (1) + glycerol (2)) at p = 0.1 MPa as a function of temperature. [a]

T / K	ρ / (kg·m^{-3})	u / (m·s^{-1})	κ_S / TPa^{-1}	n_D	R_m / (cm^3·mol^{-1})	σ / (mN·m^{-1})	$C_{p.m}$ / (J·mol·K^{-1})	ν / (mm^2· s^{-1})	η / (mPa·s)	κ/ (mS·cm^{-1})
					x_1 = 0.333					
278.15	1207.05	2049.58	197.22			68.01	211.5	1252	1511	0.260
280.65	1205.60	2042.81	198.76			67.90	212.5	1004	1211	0.320
283.15	1204.20	2036.25	200.28	1.48809	25.828	67.77	213.5	815.8	982.4	0.406
285.65	1202.80	2029.92	201.77	1.48750	25.832	67.65	214.5	666.3	801.5	0.491
288.15	1201.40	2023.98	203.19	1.48698	25.839	67.50	215.0	548.0	658.4	0.587
290.65	1200.00	2018.22	204.59	1.48632	25.840	67.34	216.0	453.1	543.7	0.703
293.15	1198.55	2012.56	205.99	1.48574	25.844	67.20	217.0	377.6	452.6	0.839
295.65	1197.15	2006.90	207.40	1.48514	25.847	67.10	217.5	316.2	378.5	0.992
298.15	1195.75	2001.29	208.81	1.48455	25.851	66.95	218.5	267.3	319.7	1.17
300.65	1194.30	1995.75	210.22	1.48396	25.855	66.81	219.0	227.3	271.4	1.36
303.15	1192.90	1990.23	211.64	1.48337	25.858	66.70	220.0	194.6	232.1	1.58
305.65	1191.50	1984.72	213.06	1.48278	25.862	66.57	221.0	167.0	199.0	1.82
308.15	1190.15	1979.24	214.49	1.48218	25.864	66.43	221.5	144.2	171.6	2.10
310.65	1188.75	1973.77	215.93	1.48159	25.866	66.31	222.5	125.3	149.0	2.40
313.15	1187.40	1968.30	217.38	1.48098	25.868	66.18	223.5	109.4	130.0	2.76
315.65	1186.00	1962.85	218.84	1.48040	25.872	66.05	224.0	95.97	113.8	3.14
318.15	1184.65	1957.38	220.32	1.47980	25.874	65.93	225.0	84.42	100.0	3.52
320.65	1183.25	1951.84	221.84	1.47921	25.877	65.74	226.0	74.73	88.43	3.94
323.15	1181.90	1946.29	223.36	1.47860	25.879	65.62	227.0	66.33	78.39	4.39
325.65	1180.50	1940.73	224.91	1.47801	25.882	65.48	228.0	58.84	69.46	4.87
328.15	1179.10	1935.15	226.47	1.47741	25.885	65.38	228.5	52.63	62.06	5.44
330.65	1177.70	1929.61	228.04	1.47681	25.888	65.23	229.0	47.23	55.63	6.03
333.15	1176.35	1924.08	229.63	1.47622	25.891	65.10	230.0	42.55	50.05	6.62
335.65	1174.95	1918.48	231.24	1.47564	25.894	64.97	231.0	38.46	45.19	7.29
338.15	1173.55	1912.86	232.88	1.47504	25.897	64.84	232.0	34.89	40.94	8.01

[a] Standard uncertainties u are $u(T)$ = 0.005 K for density and speed of sound and $u(T)$ = 0.01 K for the rest of properties, $u(p)$ = 1 kPa, and $u(x_i)$ = 0.01, and the combined expanded uncertainties U_c are $U_c(\rho)$ = 0.5 kg·m^{-3}, $U_c(u)$ = 0.5 m·s^{-1}, $U_c(n_D)$ = 10^{-4}, $U_c(\sigma)$ = 0.2 mN·m^{-1}, $U_c(C_{p,m})$ = 1 %, $U_c(\nu)$ = 2 %, $U_c(\eta)$ = 2 %, $U_c(\kappa)$ = 2 %, with 0.95 level of confidence (k=2).

Table S2. Experimental and derived thermophysical properties of glycelinewater (choline chloride (1) + glycerol (2) + water (3)) at p = 0.1 MPa as a function of temperature. [a]

T / K	ρ / (kg·m^{-3})	u / (m·s^{-1})	κ_S / TPa^{-1}	n_D	R_m / (cm^3·mol^{-1})	σ / (mN·m^{-1})	$C_{p.m}$ / (J·mol·K^{-1})	ν / (mm^2· s^{-1})	η / (mPa·s)	κ/ (mS·cm^{-1})
					x_1 = 0.249, x_2 = 0.496					
278.15	1193.60	2047.31	199.88			69.43	181.5	497.7	594.0	0.610
280.65	1192.20	2041.95	201.17			69.31	182.5	409.4	488.1	0.757
283.15	1190.80	2036.65	202.45	1.48158	20.444	69.19	183.0	339.6	404.4	0.928
285.65	1189.40	2031.43	203.74	1.48104	20.448	69.06	184.0	283.4	337.0	1.12
288.15	1188.00	2026.29	205.01	1.48048	20.452	68.92	185.0	237.6	282.3	1.35
290.65	1186.60	2021.21	206.29	1.47991	20.456	68.78	186.0	201.0	238.6	1.60
293.15	1185.20	2016.20	207.56	1.47934	20.459	68.64	186.5	171.3	203.0	1.89
295.65	1183.85	2011.14	208.84	1.47877	20.461	68.51	187.0	145.8	172.6	2.20
298.15	1182.50	2006.05	210.14	1.47818	20.463	68.39	188.0	125.0	147.8	2.55
300.65	1181.15	2001.01	211.44	1.47761	20.466	68.26	189.0	108.4	128.0	2.93
303.15	1179.80	1995.95	212.76	1.47702	20.467	68.14	190.0	94.32	111.3	3.35
305.65	1178.45	1990.88	214.10	1.47644	20.470	68.00	191.0	82.42	97.13	3.81
308.15	1177.05	1985.83	215.44	1.47586	20.473	67.87	191.5	72.43	85.25	4.30
310.65	1175.70	1980.76	216.79	1.47528	20.475	67.77	192.0	63.91	75.14	4.84
313.15	1174.30	1975.66	218.17	1.47470	20.477	67.65	193.0	56.61	66.48	5.41
315.65	1172.95	1970.54	219.56	1.47410	20.479	67.55	194.0	50.31	59.01	6.02
318.15	1171.55	1965.43	220.96	1.47353	20.482	67.44	195.0	44.90	52.61	6.67
320.65	1170.20	1960.48	222.34	1.47294	20.484	67.31	195.5	40.27	47.12	7.36
323.15	1168.80	1955.06	223.84	1.47235	20.487	67.17	196.5	36.35	42.48	8.08
325.65	1167.40	1949.80	225.32	1.47176	20.489	67.03	197.5	32.79	38.28	8.85
328.15	1166.05	1944.55	226.80	1.47117	20.491	66.90	198.0	29.72	34.66	9.66
330.65	1164.65	1939.28	228.31	1.47059	20.494	66.79	199.0	27.02	31.47	10.5
333.15	1163.25	1934.02	229.83	1.47000	20.496	66.65	199.5	24.64	28.66	11.4
335.65	1161.90	1928.52	231.42	1.46940	20.498	66.52	200.5	22.50	26.14	12.3
338.15	1160.55	1923.52	232.89	1.46881	20.500	66.39	201.0	20.62	23.94	13.3

[a] Standard uncertainties u are $u(T)$ = 0.005 K for density and speed of sound and $u(T)$ = 0.01 K for the rest of properties, $u(p)$ = 1 kPa, and $u(x_i)$ = 0.01, and the combined expanded uncertainties U_c are $U_c(\rho)$ = 0.5 kg·m^{-3}, $U_c(u)$ = 0.5 m·s^{-1}, $U_c(n_D)$ = 10^{-4}, $U_c(\sigma)$ = 0.2 mN·m^{-1}, $U_c(C_{p,m})$ = 1 %, $U_c(\nu)$ = 2 %, $U_c(\eta)$ = 2 %, $U_c(\kappa)$ = 1 %, with 0.95 level of confidence (k=2).

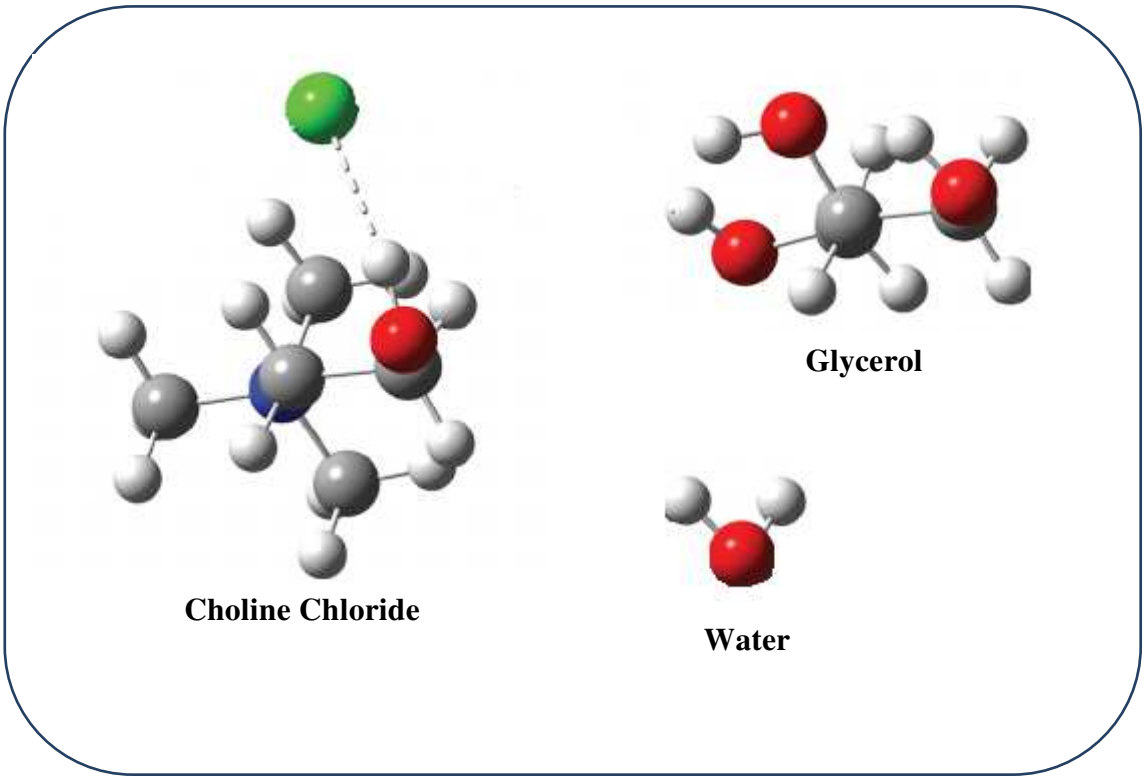

Figure S1. Chemical structures of the compounds used in this work. Atoms are colored according to type: C (gray), H (white), O (red), N (blue), and Cl (green).

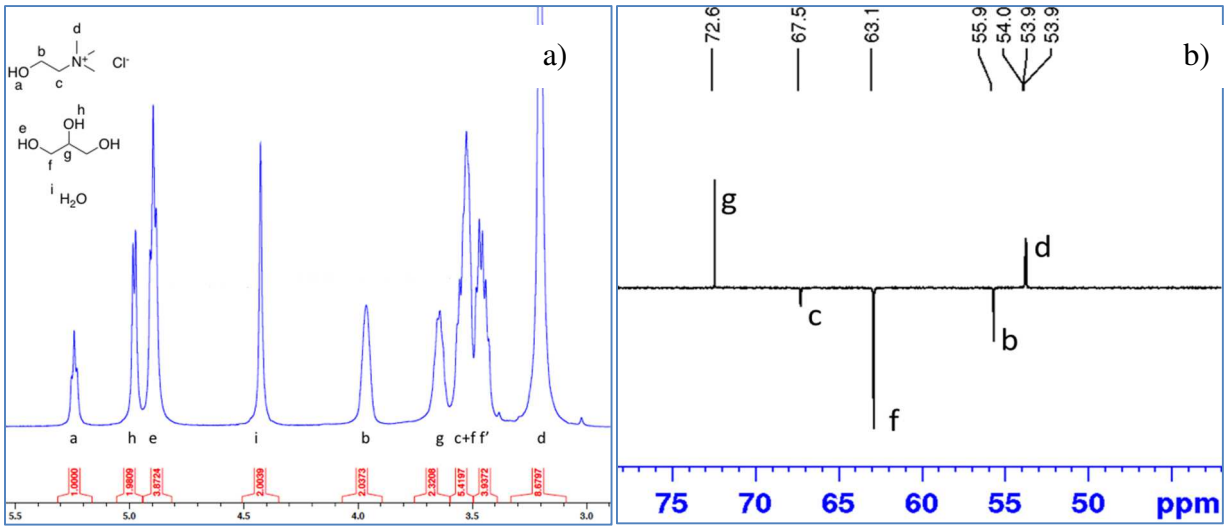

Figure S2. GlyW (1:2:1) spectra at T = 298.15 K: (a) ^{1}H-NMR 400 MHz. δ 3.04 (s, 9 H, H_d), 3.23-3.33 (m, 4 H, H_f), 3.33-3.43 (m, 6 H, H, H_c), 3.44-3.53 (m, 2 H, H_g), 3.76-3.85 (m, 2 H, H_b), 4.26 (s, 2.0 H, H_i), 4.73 (t, J = 5.0 Hz, 4 $H_{f'}$, H_e), 4.82 (d, J = 4.8 Hz, 2 H, H_h), 5.08 (t, J = 4.7 Hz, 1 H, H_a); (b) ^{13}C-NMR 100 MHz. δ 53.9 (t, J = 3.0 Hz, C_d), 55.9 (C_b), 63.1 (C_f), 67.5 (C_c), 72.6 (C_g).